DOI: 10.1021/ic901791f

Inorganic Chemistry
Article

Photocytotoxic Lanthanum(III) and Gadolinium(III) Complexes of Phenanthroline Bases Showing Light-Induced DNA Cleavage Activity

Akhtar Hussain,[†] Debojyoti Lahiri,[†] Mohammed S. Ameerunisha Begum,[†] Sounik Saha,[†] Ritankar Majumdar,[‡] Rajan R. Dighe,[‡] and Akhil R. Chakravarty*[,†]

[†]*Department of Inorganic and Physical Chemistry and* [‡]*Department of Molecular Reproduction, Development, and Genetics, Indian Institute of Science, Bangalore 560012, India*

Received September 8, 2009

Lanthanide complexes of formulation $[La(B)_2(NO_3)_3]$ (**1**−**3**) and $[Gd(B)_2(NO_3)_3]$ (**4**−**6**), where B is a *N,N*-donor phenanthroline base, namely, 1,10-phenanthroline (phen in **1**, **4**), dipyrido[3,2-*d*:2′,3′-*f*]quinoxaline (dpq in **2**, **5**) and dipyrido[3,2-*a*:2′,3′-*c*]phenazine (dppz in **3**, **6**), have been prepared, characterized from physicochemical data, and their photoinduced DNA and protein cleavage activity studied. The photocytotoxicity of the dppz complexes **3** and **6** has been studied using HeLa cancer cells. The complexes exhibit ligand centered bands in the UV region. The dppz complexes show the lowest energy band at 380 nm in *N,N*-dimethylformamide (DMF). The La(III) complexes are diamagnetic. The Gd(III) complexes (**4**−**6**) have magnetic moments that correspond to seven unpaired electrons. The complexes are 1:1 electrolytic in aqueous DMF. The dpq and dppz complexes in DMF show ligand-based reductions. The complexes display moderate binding propensity to calf thymus DNA giving binding constant values in the range of 5.7×10^4−5.8×10^5 M^{-1} with a relative order: **3**, **6** (dppz) > **2**, **5** (dpq) > **1**, **4** (phen). The binding data suggest DNA surface and/or groove binding nature of the complexes. The complexes do not show any hydrolytic cleavage of plasmid supercoiled pUC19 DNA. The dpq and dppz complexes efficiently cleave SC DNA to its nicked circular form on exposure to UV-A light of 365 nm at nanomolar complex concentration. Mechanistic studies reveal the involvement of singlet oxygen ($^1O_2$) and hydroxyl radical ($HO^•$) as the cleavage active species. The complexes show binding propensity to bovine serum albumin (BSA) protein giving K_{BSA} values of $\sim 10^5$ M^{-1}. The dppz complexes **3** and **6** show BSA protein cleavage activity in UV-A light of 365 nm. The dppz complexes **3** and **6** exhibit significant photocytotoxicity in HeLa cells giving respective IC_{50} values of 341 nM and 573 nM in UV-A light of 365 nm for an exposure time of 15 min (IC_{50} > 100 μM in dark for both the complexes). Control experiments show significant dark and phototoxicity of the dppz base alone (IC_{50} = 413 nM in light with 4 h incubation in dark and 11.6 μM in dark with 24 h incubation). A significant decrease in the dark toxicity of the dppz base is observed on binding to the lanthanide ions while retaining similar phototoxicity.

Introduction

Metal complexes that bind and cleave DNA and proteins under physiological conditions are of current interests for their varied applications in nucleic acid and protein chemistry, namely, as models for restriction enzymes, footprinting agents, model proteases, and therapeutic agents.[1−10] DNA cleavage could proceed via hydrolytic or oxidative pathways. Hydrolytic cleavage of DNA involves hydrolysis of the phosphodiester bond generating fragments that could be rejoined making the compounds as models for restriction enzymes having utility in genomic research. Ln(III), Zn(II), and Cu(II) complexes have been extensively studied for hydrolytic cleavage of DNA because of high Lewis acidity of these metal ions.[3,4] Oxidative cleavage of DNA generally

*To whom correspondence should be addressed. E-mail: arc@ipc.iisc.ernet.in. Phone: +91-80-22932533. Fax: +91-80-23600683.

(1) (a) Sigman, D. S.; Mazumder, A.; Perrin, D. M. *Chem. Rev.* **1993**, *93*, 2295. (b) Sigman, D. S.; Bruice, T. W.; Mazumder, A.; Sutton, C. L. *Acc. Chem. Res.* **1993**, *26*, 98.
(2) (a) Burrows, C. J.; Muller, J. G. *Chem. Rev.* **1998**, *98*, 1109. (b) Meunier, B. *Chem. Rev.* **1992**, *92*, 1411.
(3) (a) Cowan, J. A. *Curr. Opin. Chem. Biol.* **2001**, *5*, 634. (b) Hegg, E. L.; Burstyn, J. N. *Coord. Chem. Rev.* **1998**, *173*, 133. (c) Molenveld, P.; Engbersen, J. F. J.; Reinhoudt, D. N. *Chem. Soc. Rev.* **2000**, *29*, 75.
(4) (a) Komiyama, M.; Takida, N.; Shigekawa, H. *Chem. Commun.* **1999**, 1443. (b) Franklin, S. J. *Curr. Opin. Chem. Biol.* **2001**, *5*, 201. (c) Liu, C.; Wang, M.; Zhang, T.; Sun, H. *Coord. Chem. Rev.* **2004**, *248*, 147.
(5) (a) Boerner, L. K. J.; Zaleski, J. M. *Curr. Opin. Chem. Biol.* **2005**, *9*, 135. (b) Maurer, T. D.; Kraft, B. J.; Lato, S. M.; Ellington, A. D.; Zaleski, J. M. *Chem. Commun.* **2000**, 69.
(6) Chifotides, H. T.; Dunbar, K. R. *Acc. Chem. Res.* **2005**, *38*, 146.
(7) Garrison, W. M. *Chem. Rev.* **1987**, *87*, 381.
(8) Meggers, E. *Chem. Commun.* **2009**, 1001.
(9) (a) Zhu, L.; Kostic, N. M. *Inorg. Chim. Acta* **2002**, *339*, 104. (b) Polzin, G. M.; Burstyn, J. N. *Met. Ions. Biol. Syst.* **2001**, *38*, 103.
(10) (a) Komiyama, M. *Met. Ions Biol. Syst.* **2001**, *38*, 25. (b) Takarada, T.; Yashiro, M.; Komiyama, M. *Chemistry* **2001**, *6*, 3906. (c) Buckingham, D. A.; Clark, C. R. *Met. Ions Biol. Syst.* **2001**, *38*, 43.

Published on Web 04/09/2010

causes degradation of the sugar and/or base moiety thus making the process suitable for foot-printing and therapeutic applications. Transition metal complexes with their tunable coordination environments and versatile redox and spectral properties have been used for oxidative cleavage of DNA and as models for the chemotherapeutic agents, namely, iron-bleomycins (FeBLMs).[11−13] Besides DNA cleaving agents, the chemistry of compounds showing protein cleavage activity has received considerable current interests toward designing complexes that could show site-specific protein cleavage or could target cellular kinases that are expressed in the malignant tumor cells causing metastasis.[14−17] The anti-metastasis agents are required to target the enzymes belonging to the protein kinase family. Half-sandwich (η^6-arene)-ruthenium(II) complexes and *trans*-[tetrachlorobis(1*H*-indazole)ruthenate(III)] are known to show potent antimetastasis properties.[18,19] Further, there are reports on complexes showing hydrolytic cleavage of proteins.[20−22] The complexes showing oxidative cleavage of proteins are relatively rare.[23−25]

Oxidative cleavage of DNA by metal complexes can be achieved in the presence of external reagents or on photoactivation. Photocleavage of DNA is of importance for its potential phototherapeutic applications as an emerging non-invasive treatment modality of cancer.[26−29] The photodrug Photofrin which is an oligomeric mixture of hematoporphyrin species, undergoes photoactivation at 633 nm to generate a $^1(\pi-\pi^*)$ state with subsequent conversion to a $^3(\pi-\pi^*)$ state that activates molecular oxygen to form cytotoxic singlet oxygen. The PDT agents based on metalloenediynes are known to produce diradical intermediates upon photoactivation.[30] Non-porphyrinic organic dyes have been used as potent photocytotoxic agents.[31−34] Use of metal-based agents showing photocytotoxicity is relatively new. Turro and co-workers have reported a ruthenium(II) complex as a cisplatin analogue that binds to DNA in a similar manner as cisplatin upon photoactivation and a rhodium(II) complex that shows significant photocytotoxicity toward Hs-27 human skin cells.[35] There are few reports on platinum(IV), ruthenium(II), and rhodium(II) complexes showing photocytotoxicity.[36−39] The reports from our laboratory have shown that iron(III) and oxovanadium(IV) complexes could be designed as 3d metal-based PDT agents showing photocytotoxicity in visible light.[40,41] The present work stems from our interest to design and study the photoinduced DNA cleavage activity of lanthanide complexes. The lanthanide complexes with their varied coordination geometries could be suitably designed to achieve oxidative DNA cleavage activity. The Ln(III) complexes with their redox stability are expected to show poor chemical nuclease activity in the presence of cellular thiols. The hydrolytic DNA cleavage activity of Ln(III) complexes could be controlled with suitable design of the complexes to

(11) (a) Burger, R. M. *Chem. Rev.* **1998**, *98*, 1153. (b) Wolkenberg, S. E.; Boger, D. L. *Chem. Rev.* **2002**, *102*, 2477.
(12) (a) Thomas, C. J.; McCormick, M. M.; Vialas, C.; Tao, Z.-F.; Leitheiser, C. J.; Rishel, M. J.; Wu, X.; Hecht, S. M. *J. Am. Chem. Soc.* **2002**, *124*, 3875. (b) Rishel, M. J.; Thomas, C. J.; Tao, Z.-F.; Vialas, C.; Leitheiser, C. J.; Hecht, S. M. *J. Am. Chem. Soc.* **2003**, *125*, 10194.
(13) (a) Hertzberg, R. P.; Dervan, P. B. *J. Am. Chem. Soc.* **1982**, *104*, 313. (b) Mukherjee, A.; Dhar, S.; Nethaji, M.; Chakravarty, A. R. *Dalton Trans.* **2005**, 349.
(14) Kumar, C. V.; Buranaprapuk, A.; Thota, J. *Proc. Indian Acad. Sci.: Chem. Sci.* **2002**, *114*, 579.
(15) (a) Suh, J.; Chei, W. S. *Curr. Opin. Chem. Biol.* **2008**, *12*, 207. (b) Suh, J. *Acc. Chem. Res.* **1992**, *25*, 273.
(16) (a) Pacor, S.; Zorzet, S.; Cocchietto, M.; Bacac, M.; Vadori, M.; Turrin, C.; Gava, B.; Castellarin, A.; Sava, G. *J. Pharmacol. Exp. Ther.* **2004**, *310*, 737. (b) Sava, G.; Capozzi, I.; Clerici, K.; Gagliardi, R.; Alessio, E.; Mestroni, G. *Clin. Exp. Metastasis* **1998**, *16*, 371. (c) Scolaro, C.; Bergamo, A.; Brescacin, L.; Delfino, R.; Cocchietto, M.; Laurenczy, G.; Geldbach, T. J.; Sava, G.; Dyson, P. J. *J. Med. Chem.* **2005**, *48*, 4161.
(17) (a) Liu, H.-K.; Berners-Price, S. J.; Wang, F.; Parkinson, J. A.; Xu, J.; Bella, J.; Sadler, P. J. *Angew. Chem., Int. Ed.* **2006**, *45*, 8153. (b) Yan, Y. K.; Melchart, M.; Habtemariam, A.; Sadler, P. J. *Chem. Commun.* **2005**, 4764.
(18) Dale, L. D.; Tocher, J. H.; Dyson, T. M.; Edwards, D. I.; Tocher, D. A. *Anti-Cancer Drug Des.* **1992**, *7*, 3.
(19) Hoeschele, J. D.; Habtemariam, A.; Muir, J.; Sadler, P. J. *Dalton Trans.* **2007**, 4974.
(20) Rajendiran, V.; Palaniandavar, M.; Swaminathan, P.; Uma, L. *Inorg. Chem.* **2007**, *46*, 10446.
(21) (a) de Oliveira, M. C. B.; Scarpellini, M.; Neves, A.; Terenzi, H.; Bortoluzzi, A. J.; Szpoganics, B.; Greatti, A.; Mangrich, A. S.; Souza, E. M. De; Fernandez, P. M.; Soares, M. R. *Inorg. Chem.* **2005**, *44*, 921. (b) Kumar, C. V.; Buranaprapuk, A.; Cho, A.; Chaudhari, A. *Chem. Commun.* **2000**, 597.
(22) (a) Zhu, L.; Kostić, N. M. *J. Am. Chem. Soc.* **1993**, *115*, 4566. (b) Parac, T. N.; Kostić, N. M. *J. Am. Chem. Soc.* **1996**, *118*, 51. (c) Milović, N. M.; Dutcă, L.-M.; Kostić, N. M. *Inorg. Chem.* **2003**, *42*, 4036. (d) Milović, N. M.; Dutcă, L.-M.; Kostic, N. M. *Chem.—Eur. J.* **2003**, *9*, 5097.
(23) (a) Kumar, C. V.; Buranaprapuk, A.; Opiteck, G. J.; Moyer, M. B.; Jockusch, S.; Turro, N. J. *Proc. Natl. Acad. Sci. U.S.A.* **1998**, *95*, 10361. (b) Buranaprapuk, A.; Leach, S. P.; Kumar, C. V.; Bocarsly, J. R. *Biochim. Biophys. Acta* **1998**, *1387*, 309. (c) Kumar, C. V.; Thota, J. *Inorg. Chem.* **2005**, *44*, 825.
(24) (a) Tanimoto, S.; Matsumura, S.; Toshima, K. *Chem. Commun.* **2008**, 3678. (b) Suzuki, A.; Hasegawa, M.; Ishii, M.; Matsumura, S.; Toshima, K. *Bioorg. Med. Chem. Lett.* **2005**, *15*, 4624. (c) Suzuki, A.; Tsumura, K.; Tsuzuki, T.; Matsumura, S.; Toshima, K. *Chem. Commun.* **2007**, 4260.
(25) Roy, M.; Bhowmick, T.; Santhanagopal, R.; Ramakumar, S.; Chakravarty, A. R. *Dalton Trans.* **2009**, 4671.
(26) Bonnett, R. *Chemical Aspects of Photodynamic Therapy*; Gordon & Breach: London, U.K., 2000.
(27) Henderson, B. W.; Busch, T. M.; Vaughan, L. A.; Frawley, N. P.; Babich, D.; Sosa, T. A.; Zollo, J. D.; Dee, A. S.; Cooper, M. T.; Bellnier, D. A.; Greco, W. R.; Oseroff, A. R. *Cancer Res.* **2000**, *60*, 525.
(28) Detty, M. R.; Gibson, S. L.; Wagner, S. J. *J. Med. Chem.* **2004**, *47*, 3897.
(29) (a) Ali, H.; Van Lier, J. E. *Chem. Rev.* **1999**, *99*, 2379. (b) Kar, M.; Basak, A. *Chem. Rev.* **2007**, *107*, 2861. (c) Henderson, B. W.; Dougherty, T. J. *Photochem. Photobiol.* **1992**, *55*, 145.
(30) Bhattacharyya, S.; Zaleski, J. M. *Curr. Top. Med. Chem.* **2004**, *4*, 1637.
(31) (a) Sessler, J. L.; Hemmi, G.; Mody, T. D.; Murai, T.; Burrell, A.; Young, S. W. *Acc. Chem. Res.* **1994**, *27*, 43. (b) Wei, W.-H.; Wang, Z.; Mizuno, T.; Cortez, C.; Fu, L.; Sirisawad, M.; Naumovski, L.; Magda, D.; Sessler, J. L. *Dalton Trans.* **2006**, 1934. (c) Mao, J.; Zhang, Y.; Zhu, J.; Zhang, C.; Guo, Z. *Chem. Commun.* **2009**, 908.
(32) (a) Ramaiah, D.; Eckert, I.; Arun, K. T.; Weidenfeller, L.; Epe, B. *Photochem. Photobiol.* **2004**, *79*, 99. (b) Ramaiah, D.; Eckert, I.; Arun, K. T.; Weidenfeller, L.; Epe, B. *Photochem. Photobiol.* **2002**, *76*, 672.
(33) (a) Pandey, R. K.; Sumlin, A. B.; Constantine, S.; Aoudia, M.; Potter, W. R.; Bellnier, D. A.; Henderson, B. W.; Rodgers, M. A.; Smith, K. M.; Dougherty, T. J. *Photochem. Photobiol.* **1996**, *64*, 194. (b) Sternberg, E. D.; Dolphin, D.; Brückner, C. *Tetrahedron* **1998**, *54*, 4151. (c) Nelson, J. S.; Roberts, W. G.; Berns, J. M. *Cancer Res.* **1987**, *47*, 4681. (d) Bonnett, R.; White, R. D.; Winfield, U.-J.; Berenbaum, M. C. *Biochem. J.* **1989**, *261*, 277.
(34) Atilgan, S.; Ekmeckci, Z.; Dogan, A. L.; Guc, D.; Akkaya, E. U. *Chem. Commun.* **2006**, 4398.
(35) (a) Singh, T. N.; Turro, C. *Inorg. Chem.* **2004**, *43*, 7260. (b) Lutterman, D. A.; Fu, P. K.-L.; Turro, C. *J. Am. Chem. Soc.* **2006**, *128*, 738.
(36) Mackay, F. S.; Woods, J. A.; Heringová, P.; Kašpárková, J.; Pizarro, A. M.; Moggach, S. A.; Parsons, S.; Brabec, V.; Sadler, P. J. *Proc. Natl. Acad. Sci. U.S.A.* **2007**, *104*, 20743.
(37) Rose, M. J.; Fry, N. L.; Marlow, R.; Hinck, L.; Mascharak, P. K. *J. Am. Chem. Soc.* **2008**, *130*, 8834.
(38) Angeles-Boza, A. M.; Chifotides, H. T.; Aguirre, J. D.; Chouai, A.; Fu, P. K.-L.; Dunbar, K. R.; Turro, C. *J. Med. Chem.* **2006**, *49*, 6841.
(39) Brindell, M.; Kuliś, E.; Elmroth, S. K.; Urbańska, K.; Stochel, G. *J. Med. Chem.* **2005**, *48*, 7298.
(40) (a) Roy, M.; Saha, S.; Patra, A. K.; Nethaji, M.; Chakravarty, A. R. *Inorg. Chem.* **2007**, *46*, 4368. (b) Saha, S.; Majumdar, R.; Roy, M.; Dighe, R. R.; Chakravarty, A. R. *Inorg. Chem.* **2009**, *48*, 2652.
(41) Sasmal, P. K.; Saha, S.; Majumdar, R.; Dighe, R. R.; Chakravarty, A. R. *Chem. Commun.* **2009**, 1703.

minimize cellular dark toxicity. While there are few literature reports on the lanthanide complexes showing DNA binding propensity, the study on photoinduced DNA cleavage activity of lanthanide complexes is relatively unexplored except some lanthanide complexes of macrocyclic organic dyes. For example, the Gd(III) and Lu(III) complexes of texaphyrins have been studied as photodynamic therapy (PDT) agents with the lutetium(III) texaphyrin (LUTRIN) showing PDT effect in near-IR light of 732 nm.[42,43] The major biomedical applications of the lanthanide complexes are directed toward magnetic resonance imaging (MRI) of cancer.[44−47] The Gd(III)-based complexes, namely, $[Gd(DTPA)(H_2O)]^{2-}$ (Magnevist) and $[Gd(DOTA)(H_2O)]^{-}$ (Dotarem) are currently used as clinical MRI agents.[47] It would be of immense interest to develop the chemistry of lanthanide complexes showing dual functionality as MRI and PDT agents.

To explore the photoinduced DNA and protein cleavage activity of La(III) and Gd(III) complexes, we have used photoactive planar phenanthroline bases like dipyridoquinoxaline (dpq) and dipyridophenazine (dppz). The dpq and dppz ligands are known to generate photoexcited $^3(n-\pi^*)$ and/or $^3(\pi-\pi^*)$ state cleaving DNA on photoirradiation with high energy UV light.[48] Binding of these ligands to metal ions could significantly augment their DNA photocleavage activity in low-energy UV-A light. Parker and coworkers have recently shown that lanthanide complexes of a nonadentate ligand having a covalently attached dpq moiety exhibit UV light-induced plasmid DNA cleavage activity.[49] A mechanism based on a Ln^{4+} transient intermediate is proposed for the DNA cleavage reaction. We have synthesized and characterized lanthanide complexes $[La(B)_2(NO_3)_3]$ (**1**−**3**) and $[Gd(B)_2(NO_3)_3]$ (**4**−**6**), where B is a *N,N*- donor phenanthroline base, namely, 1,10-phenanthroline (phen in **1, 4**), dipyrido[3,2-*d*:2′,3′-*f*]quinoxaline (dpq in **2, 5**) and dipyrido[3,2-a:2′,3′-*c*]phenazine (dppz in **3, 6**), to study their photoinduced DNA cleavage activity and the mechanistic pathways involved in the DNA cleavage reactions (Scheme 1). We have observed the presence of dual mechanistic pathways involving type-II and photoredox processes in the DNA photocleavage reactions. Significant results of this report include observation of efficient photoinduced DNA cleavage activity of the dpq and dppz complexes at nanomolar concentrations and significant reduction of the cellular dark toxicity of the dppz base on binding to the lanthanide ions.

Scheme 1. Complexes **1**−**6** and the Phenanthroline Bases Used

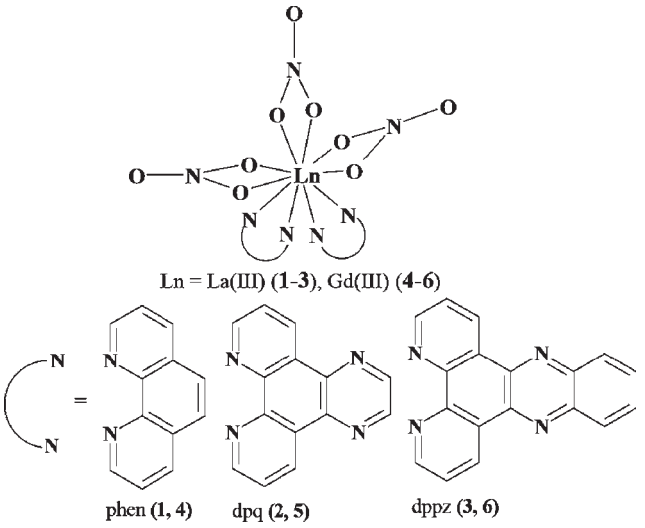

Experimental Section

Materials and Methods. All the reagents and chemicals were procured from commercial sources (SD Fine Chemicals, India; Aldrich, U.S.A.) and used without any further purification. Solvents used were purified by standard procedures.[50] Supercoiled (SC) pUC19 DNA (cesium chloride purified) was purchased from Bangalore Genie (India). Tris-(hydroxymethyl)-aminomethane-HCl (Tris-HCl) buffer solution was prepared using deionized and sonicated triple distilled water using a quartz water distillation setup. Calf thymus (CT) DNA, agarose (molecular biology grade), distamycin-A, methyl green, catalase, superoxide dismutase (SOD), 2,2,6,6-tetramethyl-4-piperidone (TEMP), 1,4-diazabicyclo[2.2.2]octan (DABCO), ethidium bromide (EB), Hoechst 33258, bovine serum albumin (BSA) protein, acrylamide, *N,N*′-methylene-bis-acrylamide, ammonium persulphate, *N,N,N*′,*N*′-tetramethylethylenediamine (TEMED), 2-mercaptoethanol (MPE), glycerol, sodium dodecyl sulfate (SDS), bromophenol blue, coomassie brilliant blue R-250 were from Sigma (U.S.A.). The *N,N*-donor heterocyclic bases dipyrido-[3,2-*d*:2′,3′-*f*]-quinoxaline and dipyrido[3,2-*a*:2′,3′-*c*]-phenazine were prepared by literature procedures using 1,10-phenanthroline-5,6-dione as a precursor reacted with ethylenediamine for dpq and 1,2-phenylenediamine for dppz.[51,52]

The elemental analyses were done using a Thermo Finnigan Flash EA 1112 CHNS analyzer. The infrared spectra were recorded on a Bruker ALPHA FT-IR spectrometer. Electronic spectra were recorded on a PerkinElmer Spectrum one 55 spectrophotometer. Molar conductivity measurements were performed using a Control Dynamics (India) conductivity meter. Room temperature magnetic susceptibility data for the Gd(III) complexes were obtained from a George Associates Inc. Lewis-coil force magnetometer using $Hg[Co(NCS)_4]$ as a standard. Experimental susceptibility data were corrected for diamagnetic contributions.[53] Cyclic voltammetric measurements were made at 25 °C on a EG&G PAR Model 253 VersaStat potentiostat/galvanostat with electrochemical analysis software 270 using a three electrode setup comprising a glassy carbon working, platinum wire auxiliary, and a saturated calomel reference (SCE) electrode. Tetrabutylammonium perchlorate

(42) (a) Young, S. W.; Woodburn, K. W.; Wright, M.; Mody, T. D.; Fan, Q.; Sessler, J. L.; Dow, W. C.; Miller, R. A. *Photochem. Photobiol.* **1996**, *63*, 892. (b) Guldi, D. M.; Mody, T. D.; Gerasimchuk, N. N.; Magda, D.; Sessler, J. L. *J. Am. Chem. Soc.* **2000**, *122*, 8289.
(43) Sessler, J. L.; Miller, R. A. *Biochem. Pharmacol.* **2000**, *59*, 733.
(44) (a) Werner, E. J.; Datta, A.; Jocher, C. J.; Raymond, K. N. *Angew. Chem., Int. Ed.* **2008**, *47*, 8568. (b) Datta, A.; Raymond, K. N. *Acc. Chem. Res.* **2009**, *42*, 938. (c) Major, J. L.; Meade, T. J. *Acc. Chem. Res.* **2009**, *42*, 893.
(45) (a) Caravan, P. *Acc. Chem. Res.* **2009**, *42*, 851. (b) Caravan, P. *Chem. Soc. Rev.* **2006**, *35*, 512. (c) Aime, S.; Botta, M.; Fasano, M.; Terreno, E. *Chem. Soc. Rev.* **1998**, *27*, 19.
(46) (a) Parker, D.; Dickins, R. S.; Puschmann, H.; Crossland, C.; Howard, J. A. K. *Chem. Rev.* **2002**, *102*, 1977. (b) Bottrill, M.; Kwok, L.; Long, N. J. *Chem. Soc. Rev.* **2006**, *35*, 557. (c) Ahrens, E. T.; Rothbächer, U.; Jacobs, R. E.; Fraser, S. E. *Proc. Natl. Acad. Sci. U.S.A.* **1998**, *95*, 8443.
(47) (a) Caravan, P.; Ellison, J. J.; McMurry, T. J.; Lauffer, R. B. *Chem. Rev.* **1999**, *99*, 2293. (b) Lauffer, R. B. *Chem. Rev.* **1987**, *87*, 901.
(48) Toshima, K.; Takano, R.; Ozawa, T.; Matsumura, S. *Chem. Commun.* **2002**, 212.
(49) Frias, J. C.; Bobba, G.; Cann, M. J.; Hutchison, C. J.; Parker, D. *Org. Biomol. Chem.* **2003**, *1*, 905.
(50) Perrin, D. D.; Armarego, W. L. F.; Perrin, D. R. *Purification of Laboratory Chemicals*; Pergamon Press: Oxford, 1980.
(51) (a) Dickeson, J. E.; Summers, L. A. *Aus. J. Chem.* **1970**, *23*, 1023. (b) Collins, J. G.; Sleeman, A. D.; Aldrich-Wright, J. R.; Greguric, I.; Hambley, T. W. *Inorg. Chem.* **1998**, *37*, 3133.
(52) Amouyal, E.; Homsi, A.; Chambron, J.-C.; Sauvage, J.-P. *J. Chem. Soc., Dalton Trans.* **1990**, 1841.
(53) Kahn, O. *Molecular Magnetism*; VCH: Weinheim, 1993.

(TBAP, 0.1 M) was used as a supporting electrolyte in DMF. The electrochemical data were uncorrected for junction potentials. Electrospray ionization mass spectral measurements were done using Bruker Daltonics make (Esquire 300 Plus ESI Model). Mass spectral measurements of BSA samples were done using Bruker Daltonics Ultraflex MALDI-TOF instrument. ^{1}H NMR spectra of the ligands and the La(III) complexes were recorded at room temperature on a Bruker 400 MHz NMR spectrometer.

Synthesis of [La(B)$_2$(NO$_3$)$_3$] (1−3) and [Gd(B)$_2$(NO$_3$)$_3$] (4−6) [B = phen (in 1, 4); dpq (in 2, 5), dppz (in 3, 6)]. The complexes **1**−**6** were prepared by following a reported synthetic procedure in modified form in which a hot ethanolic solution of Ln(NO$_3$)$_3$·6H$_2$O (Ln = La(III), 0.433 g; Gd(III), 0.451 g; 1.0 mmol) in boiling ethanol (30 mL) was added dropwise to a stirred solution of the respective heterocyclic base B (0.40 g phen; 0.47 g dpq; 0.57 g dppz; 2.0 mmol) in boiling ethanol (30 mL).[54] After stirring for 5 min, a crystalline precipitate was obtained. The solid was isolated, washed with 20 mL of hot ethanol followed by 20 mL of diethyl ether, and finally dried in vacuum over P_4O_{10} [Yield: ∼70%]. The characterization data for the complexes are given below.

[La(phen)$_2$(NO$_3$)$_3$] (1). Anal. Calcd for $C_{24}H_{18}N_7O_9La$: C, 42.06; H, 2.35; N, 14.30. Found: C, 42.32; H, 2.45; N, 14.16. ESI-MS in 10% aqueous MeOH: m/z 623 [M-NO$_3^-$]$^+$. IR data/cm^{-1}: 1620w, 1591w, 1470vs, 1408s, 1284s, 1150w, 1102w, 1027s, 862w, 843s, 816 m, 763w, 717vs, 637 m, 417 m (vs, very strong; s, strong; m, medium; w, weak). UV−visible in DMF [λ_{max}/nm (ε/ M^{-1} cm^{-1})]: 322sh (2420), 310sh (4340), 266 (66 420) (sh, shoulder). ^{1}H NMR in DMSO-d_6 (δ, ppm): 9.01 (dd, 2H, J = 8.0, 1.7 Hz), 8.4 (dd, 2H, J = 4.8, 1.6 Hz), 7.9 (s, 2H), 7.68 (dd, 2H, J = 8.2, 4.4 Hz).

[La(dpq)$_2$(NO$_3$)$_3$] (2). Anal. Calcd for $C_{28}H_{18}N_{11}O_9La$: C, 42.60; H, 2.04; N, 19.52. Found: C, 42.86; H, 2.26; N, 19.31. ESI-MS in 1:1 MeOH−MeCN mixture: m/z 727 [M-NO$_3^-$]$^+$. IR data/cm^{-1}: 1634w, 1576 m, 1460vs, 1395s, 1287vs, 1210w, 1120w, 1084 m, 1037 m, 867w, 813s, 735vs, 696w, 634w, 434w, 416 m. UV−visible in DMF [λ_{max}/nm (ε/ M^{-1} cm^{-1})]: 340 (17 700), 325sh (21 700), 265 (72 400). ^{1}H NMR in DMSO-d_6 (δ, ppm): 9.37 (dd, 2H, J = 8.3, 1.8 Hz), 9.15 (dd, 2H, J = 4.4, 1.8 Hz), 9.09 (s, 2H), 7.88 (dd, 2H, J = 8.3, 4.2 Hz).

[La(dppz)$_2$(NO$_3$)$_3$] (3). Anal. Calcd for $C_{36}H_{20}N_{11}O_9La$: C, 48.61; H, 2.27; N, 17.32. Found: C, 48.80; H, 2.29; N, 17.42. ESI-MS in 1:1 MeOH−MeCN mixture: m/z 827 [M-NO$_3^-$]$^+$. IR data/cm^{-1}: 1577 m, 1477vs, 1410s, 1361 m, 1287vs, 1135w, 1080s, 1025 m, 818s, 762s, 730vs, 703 m, 637w, 615w, 575w, 415s. UV−visible in DMF [λ_{max}/nm (ε/ M^{-1} cm^{-1})]: 380 (19 460), 369 (15 900), 362 (18 150), 351 (13 000), 294sh (30 000), 268 (72 400). ^{1}H NMR in DMSO-d_6 (δ, ppm): 9.44 (dd, 2H, J = 8.2, 1.8 Hz), 9.11 (dd, 2H, J = 4.5, 2.0 Hz), 8.29−8.33 (m, 2H), 7.95−7.99 (m, 2H), 7.85 (dd, 2H, J = 8.4, 4.0 Hz).

[Gd(phen)$_2$(NO$_3$)$_3$] (4). Anal. Calcd for $C_{24}H_{18}N_7O_9Gd$: C, 40.96; H, 2.29; N, 13.93. Found: C, 41.04; H, 2.00; N, 14.21. ESI-MS in 10% aqueous MeOH: m/z 642 [M-NO$_3^-$]$^+$. IR data/cm^{-1}: 1621w, 1590w, 1468vs, 1410s, 1290vs, 1143 m, 1099 m, 1027 m, 855s, 812 m, 765w, 717vs, 636 m, 417 m. UV−visible in DMF [λ_{max}/nm (ε/ M^{-1} cm^{-1})]: 322sh (3230), 310sh (4850), 266(68 040). μ_{eff} = 7.94 μ_B at 298 K.

[Gd(dpq)$_2$(NO$_3$)$_3$] (5). Anal. Calcd for $C_{28}H_{18}N_{11}O_9Gd$: C, 41.63; H, 2.00; N, 19.07. Found: C, 41.71; H, 2.15; N, 19.20. ESI-MS in 1:1 MeOH−MeCN mixture: m/z 746 [M-NO$_3^-$]$^+$. IR data/cm^{-1}: 1580 m, 1463vs, 1400s, 1296vs, 1215w, 1125w, 1080 m, 1027 m, 880w, 809 m, 728vs, 700 m, 637w, 430 m, 419 m. UV−visible in DMF [λ_{max}/nm (ε/ M^{-1} cm^{-1})]: 340 (17 930), 325sh (22 110), 265 (74 100). μ_{eff} = 7.98 μ_B at 298 K.

[Gd(dppz)$_2$(NO$_3$)$_3$] (6). Anal. Calcd for $C_{36}H_{20}N_{11}O_9Gd$: C, 47.63; H, 2.22; N, 16.97. Found: C, 47.84; H, 2.20; N, 16.77. ESI-MS in 1:1 MeOH−MeCN mixture: m/z 846 [M-NO$_3^-$]$^+$. IR data/cm^{-1}: 1570w, 1480vs, 1416 m, 1362 m, 1295vs, 1136w, 1073 m, 1028s, 821s, 761s, 730vs, 703s, 641w, 613w, 572w, 415s. UV−visible in DMF [λ_{max}/nm (ε/ M^{-1} cm^{-1})]: 380 (20 270), 369(17 260), 361 (19 450), 351 (14 600), 293sh (31 000), 269 (78 600). μ_{eff} = 7.96 μ_B at 298 K.

Solubility and Stability. All the complexes were soluble in DMF and DMSO. The phenanthroline complexes were soluble in H$_2$O and MeCN. The complexes showed less solubility in MeOH and EtOH. The complexes were stable in the solid state. The complexes showed decomposition on prolonged storage in the solution phase.[54] The solution stability of the dppz complex **3** ($\log\beta_2$ = 10.4) was measured in 10% aqueous DMF following a literature method (vide Supporting Information for details).[55]

DNA Binding Methods. DNA binding experiments were done in Tris-HCl/NaCl buffer (5 mM Tris-HCl, 5 mM NaCl, pH 7.2) using DMF solution of the complexes **1**−**6**. Calf thymus (CT) DNA (ca. 350 μM NP) in this buffer medium gave a ratio of UV absorbance at 260 and 280 nm of about 1.9:1 indicating that the DNA is apparently free from protein. The concentration of CT DNA was estimated from its absorption intensity at 260 nm with a known molar extinction coefficient value (ε) of 6600 M^{-1} cm^{-1}.[56] Absorption titration experiments were made by varying the concentration of the CT DNA while keeping the metal complex concentration constant. Due correction was made for the absorbance of CT DNA itself. Each spectrum was recorded after equilibration of the sample for 5 min. The intrinsic equilibrium binding constant (K_b) and the binding site size (s) of the complexes **1**−**6** to CT DNA were obtained by the McGhee−von Hippel (MvH) method using the expression of Bard et al. by monitoring the change of the absorption intensity of the spectral bands with increasing concentration of CT DNA by regression analysis using the equation $(\varepsilon_a - \varepsilon_f)/(\varepsilon_b - \varepsilon_f) = (b - (b^2 - 2K_b{}^2C_t[DNA]_t/s)^{1/2})/2K_bC_t$, where $b = 1 + K_bC_t + K_b[DNA]_t/2s$ and ε_a is the extinction coefficient observed for the absorption band at a given DNA concentration, ε_f is the extinction coefficient of the complex free in solution, ε_b is the extinction coefficient of the complex when fully bound to DNA, K_b is the equilibrium binding constant, C_t is the total metal complex concentration, $[DNA]_t$ is the DNA concentration in nucleotides, and s is the binding site size in base pairs.[57,58] The non-linear least-squares analyses were done using Origin Lab, version 6.1. The apparent DNA binding constant (K_{app}) values of the complexes **1**−**6** were obtained from fluorescence spectral measurements using ethidium bromide bound CT DNA solution in Tris-HCl/NaCl buffer (pH, 7.2). The fluorescence intensities of ethidium bromide at 600 nm (546 nm excitation) were recorded with an increasing amount of the added complex concentration. Ethidium bromide showed no apparent emission in Tris-buffer medium because of fluorescence quenching of the free ethidium bromide by the solvent molecules.[59] In the presence of CT DNA, ethidium bromide showed significantly enhanced emission intensity. The K_{app} values were obtained from the equation: $K_{app} \times [complex]_{50} = K_{EB} \times [EB]$, where K_{app} is the apparent binding constant of the complex studied, $[complex]_{50}$ is the concentration of the complex at 50% quenching of DNA-bound ethidium bromide emission intensity, K_{EB} is the binding constant of ethidium bromide (K_{EB} = 1.0 × 10^7 M^{-1}), and [EB] is the concentration of ethidium bromide (1.3 μM).[60]

(54) Hart, F. A.; Laming, F. P. *J. Inorg. Nucl. Chem.* **1965**, *27*, 1605.
(55) Vallee, B. L.; Coombs, T. L. *J. Biol. Chem.* **1959**, *234*, 2615.
(56) Reichmann, M. E.; Rice, S. A.; Thomas, C. A.; Doty, P. *J. Am. Chem. Soc.* **1954**, *76*, 3047.
(57) McGhee, J. D.; von Hippel, P. H. *J. Mol. Biol.* **1974**, *86*, 469.
(58) Carter, M. T.; Rodriguez, M.; Bard, A. J. *J. Am. Chem. Soc.* **1989**, *111*, 8901.
(59) (a) Waring, M. J. *J. Mol. Biol.* **1965**, *13*, 269. (b) LePecq, J.-B.; Paoletti, C. *J. Mol. Biol.* **1967**, *27*, 87.
(60) Lee, M.; Rhodes, A. L.; Wyatt, M. D.; Forrow, S.; Hartley, J. A. *Biochemistry* **1993**, *32*, 4237.

DNA melting experiments were carried out by monitoring the absorbance of CT DNA (200 μM) at 260 nm at various temperatures, both in the absence and presence of the complexes (20 μM). Measurements were carried out using a Cary 300 bio UV−visible spectrometer with a Cary temperature controller at an increase rate of 0.5 °C per min of the solution. Viscometric titrations were performed with a Schott Gerate AVS 310 Automated Viscometer that was thermostatted at 37 °C in a constant temperature bath. The concentration of CT DNA was 150 μM in NP (nucleotide pair), and the flow times were measured using an automated timer. Each sample was measured 3 times, and an average flow time was calculated. Data were presented as $(\eta/\eta_0)^{1/3}$ versus [complex]/[DNA], where η is the viscosity of DNA in the presence of complex and η_0 is that of DNA alone. Viscosity values were calculated from the observed flow time of DNA-containing solutions (t) corrected for that of the buffer alone (t_0), $\eta = (t - t_0)/t_0$. Due corrections were made for the viscosity of DMF solvent present in the solution.

DNA Cleavage Experiments. The cleavage of supercoiled (SC) pUC19 DNA (30 μM, 0.2 μg, 2686 base-pairs) was studied by agarose gel electrophoresis. For photoinduced DNA cleavage studies, the reactions were carried out under illuminated conditions using UV-A light of 365 nm (6 W, Model LF-206.LS of Bangalore Genei). Eppendorf vials were used for photocleavage experiments in a dark room at 25 °C using SC DNA (1 μL, 30 μM) in 50 mM Tris-HCl buffer (pH 7.2) containing 50 mM NaCl and the complex (2 μL) with varied concentrations. The concentration of the complexes in DMF or the additives in buffer corresponded to the quantity in 2 μL stock solution after dilution to the 20 μL final volume using Tris-HCl buffer. The solution path length in the sample vial was ~5 mm. After light exposure, each sample was incubated for 1.0 h at 37 °C and analyzed for the photocleaved products using gel electrophoresis. Mechanistic studies were carried out using different additives (NaN_3, 0.5 mM; TEMP, 0.5 mM; DABCO, 0.5 mM; DMSO, 4 μL; KI, 0.5 mM; catalase, 4 units; SOD, 4 units) prior to the addition of the complex. For the D_2O experiment, this solvent was used for dilution of the sample to 20 μL final volume. The samples after incubation in a dark chamber were added to the loading buffer containing 0.25% bromophenol blue, 0.25% xylene cyanol, 30% glycerol (3 μL), and the solution was finally loaded on 1% agarose gel containing 1.0 μg/mL ethidium bromide. Electrophoresis was carried out in a dark room for 2.0 h at 60 V in TAE (Tris-acetate EDTA) buffer. Bands were visualized in UV light and photographed. The extent of SC DNA cleavage was measured from the intensities of the bands using the UVITEC Gel Documentation System. Due corrections were made for the low level of nicked circular (NC) form of DNA present in the original SC DNA sample and for the low affinity of ethidium bromide binding to SC compared to NC and linear forms of DNA.[61] The observed error in measuring the band intensities was in the range 3−5%.

BSA Interaction and Cleavage Experiments. The protein interaction study was performed by tryptophan fluorescence quenching experiments using BSA (2 μM) in phosphate buffer (pH 6.8) containing 15% DMF. Quenching of the emission intensity of tryptophan residues of BSA at 344 nm (excitation wavelength at 295 nm) was monitored using complexes **1**−**6** as quenchers with increasing complex concentration.[62] Stern−Volmer I_0/I versus [complex] plots were made using the corrected fluorescence data taking into account the effect of dilution. A linear fit of the data using the equation: $I_0/I = 1 + K_{BSA}[Q]$, where I_0 and I are the respective emission intensities of BSA in absence and presence of the quencher of concentration [Q], gave the interaction constant (K_{BSA}) values using Origin 6.1.

Photoinduced BSA cleavage experiments were carried out following literature procedure.[63] Freshly prepared solutions of BSA in 50 mM Tris-HCl buffer (pH 7.2) containing 0.6% DMF were used for the photochemical protein cleavage studies. The BSA solutions in Tris-HCl buffer medium containing complexes **1**−**6** (10 μM and 15 μM) and BSA (5 μM) were photoirradiated at 365 nm (100 W) in Eppendorf vials. The BSA solutions containing the complexes were incubated at 37 °C for 1.0 h prior to the photoexposure. The photoirradiated samples (50 μL) were dried in a centrifugal vaporizer (EYELA Centrifugal Vaporizer, Model CVE-200D), and the samples were dissolved in the loading buffer (24 μL) containing SDS (7% w/v), glycerol (4% w/v), Tris-HCl buffer (50 mM, pH 6.8), mercaptoethanol (2% v/v), and bromophenol blue (0.01% w/v). The protein solutions were then denatured by heating on a boiling water bath for 3 min. The samples were loaded on a 3% polyacrylamide stacking gel. The gel electrophoresis was done at an initial applied voltage of 60 V until the dye passed into the separating gel from the stacking (3%) gel, and then the voltage was increased to 110 V. The gels were run for 1.5 h, stained with Coomassie Brilliant Blue R-250 solution (acetic acid/methanol/water = 1:2:7 v/v) and destained with water/methanol/acetic acid mixture (5:4:1 v/v) for 4 h. The gels, after destaining, were scanned with a HP Scanjet G3010 scanner, and the images were further processed using the Adobe Photoshop 7.0 software package. Molecular weight markers were used in each gel to calibrate the molecular weight of the protein. The presence of reactive oxygen species was investigated by carrying out the photoinduced protein cleavage experiments using singlet oxygen quenchers such as NaN_3 (3 mM) and TEMP (3 mM) and hydroxyl radical scavengers, namely, DMSO (20 μL) and KI (3 mM).

Cell Cytotoxicity Assay. The photocytotoxicity of the dppz complexes (**3**, **6**) and the dppz ligand was studied using 3-(4,5-dimethylthiazol-2-yl)-2,5-diphenyltetrazolium bromide (MTT) assay which is based on the ability of mitochondrial dehydrogenases of viable cells to cleave the tetrazolium rings of MTT forming dark purple membrane impermeable crystals of formazan that could be quantified at 595 nm after solubilization in detergent.[64] Approximately, 8000 cells of human cervical carcinoma (HeLa) were plated in 96 wells culture plate in Dulbecco's Modified Eagle Medium (DMEM) containing 10% FBS, and after 24 h of incubation at 37 °C in a CO_2 incubator, various concentrations of the complexes **3**, **6** or dppz ligand dissolved in 1% DMSO were added to the cells and incubation was continued for 4 h in dark. The medium was subsequently replaced with PBS and photoirradiated for 15 min using UV-A light of 365 nm. After photoexposure, PBS was removed and replaced with DMEM-FBS, and incubation was continued for further 24 h in dark. At the end of the incubation period, 20 μL of 5 mg mL^{-1} MTT was added to each well and incubated for an additional 3 h. The culture medium was finally discarded, and 100 μL of 10% SDS/0.01 M HCl was added. The plates were then incubated at 37 °C for 6 h to dissolve the formazan crystals, and the absorbance at 595 nm was determined using a BIORAD ELISA plate reader. Cytotoxicity of the dppz ligand and the complexes **3** and **6** was measured as the percentage ratio of the absorbance of the treated cells to the untreated controls. The IC_{50} values were determined by non-linear regression analysis using the GraphPad Prism software. To determine the dark cytotoxicity of the complexes **3** and **6** and the dppz ligand, various concentrations of the complexes or dppz ligand dissolved in DMSO (1%) were added to the HeLa cells and incubated for 24 h in dark, thereafter the media were discarded

(61) Bernadou, J.; Pratviel, G.; Bennis, F.; Girardet, M.; Meunier, B. *Biochemistry* **1989**, *28*, 7268.
(62) Quiming, N. S.; Vergel, R. B.; Nicolas, M. G.; Villanueva, J. A. *J. Health Sci.* **2005**, *51*, 8.
(63) Kumar, C. V.; Buranaprapuk, A.; Sze, H. C.; Jockusch, S.; Turro, N. J. *Proc. Natl. Acad. Sci. U.S.A.* **2002**, *99*, 5810.
(64) Mosmann, T. *J. Immunol. Methods* **1983**, *65*, 55.

Table 1. Physicochemical Data for the Complexes **1**−**6**

complex	IR[a], cm^{-1} (NO_3^-)	CV data [E_{pc}/V][b]	μ_{eff}[c]	Λ_M[d]/S cm^2 M^{-1}
$[La(phen)_2(NO_3)_3]$ (**1**)	1470, 1408,1284			128
$[La(dpq)_2(NO_3)_3]$ (**2**)	1460, 1395, 1287	−1.45[e]		122
$[La(dppz)_2(NO_3)_3]$ (**3**)	1477, 1410, 1287	−1.16[f]		124
$[Gd(phen)_2(NO_3)_3]$ (**4**)	1468, 1410, 1290		7.94	123
$[Gd(dpq)_2(NO_3)_3]$ (**5**)	1463, 1400, 1296	−1.48[g]	7.98	130
$[Gd(dppz)_2(NO_3)_3]$ (**6**)	1480, 1416, 1295	−1.20[h]	7.96	124

[a] In KBr phase. [b] Scan rate of 50 mV s^{-1} in DMF-0.1 M TBAP. Potentials are versus saturated calomel electrode (SCE). E_{pc} and E_{pa} are the cathodic and anodic peak potentials, respectively. The i_{pa} and i_{pc} are the peak anodic and cathodic current, respectively. [c] μ_{eff} in μ_B for solid powdered samples at 298 K. [d] Λ_M, molar conductivity in 15% aqueous DMF at 25 °C. [e] This cathodic peak shows an anodic counterpart at −0.45 V (E_{pa}) with i_{pa}/i_{pc} ratio of 0.1. [f] This cathodic peak shows three anodic counterparts at −1.07 V (E_{pa1}), −0.35 V (E_{pa2}) and −0.13 V (E_{pa3}) with i_{pa}/i_{pc} ratio of 0.5, 0.2 and 0.1, respectively. [g] This cathodic peak has two anodic counterparts at −1.44 V (E_{pa1}) and −0.65 V (E_{pa2}) with i_{pa}/i_{pc} ratio of 0.4 and 0.2, respectively. [h] This cathodic peak shows two anodic counterparts at −1.08 V (E_{pa1}) and −0.10 V (E_{pa2}) with i_{pa}/i_{pc} ratio of 0.6 and 0.3, respectively. The dppz ligand alone shows a voltammetric response at −1.15 V with a ΔE_p value of 70 mV at 50 mV s^{-1} scan rate giving an i_{pa}/i_{pc} ratio of 0.9.

and fresh media containing 10% FBS was added to the wells. MTT assay was then carried out as mentioned above. Cytotoxicity of the control species, namely, Cisplatin and $[Zn(dppz)_2(NO_3)_2]$ was studied following the above procedure.

Results and Discussion

Synthesis and General Aspects. Lanthanide(III) complexes $[La(B)_2(NO_3)_3]$ (**1**−**3**) and $[Gd(B)_2(NO_3)_3]$ (**4**−**6**) of phenanthroline bases (B), namely, 1,10-phenanthroline (phen in **1, 4**), dipyrido[3,2-*d*:2′,3′-f]quinoxaline (dpq in **2, 5**), and dipyrido[3,2-*a*:2′,3′-*c*]phenazine (dppz in **3, 6**), are prepared by a general synthetic procedure in which lanthanum(III) or gadolinium(III) nitrate hexahydrate is reacted with the corresponding phenanthroline base in boiling ethanol (Scheme 1). The complexes have been characterized from analytical and mass spectral (ESI-MS) data (Figures S1−S6 in the Supporting Information). Selected physicochemical data for the complexes are given in Table 1. The molar conductivity data show that the complexes are 1:1 electrolytic in aqueous DMF (1:1 v/v), and this is further supported from the presence of a prominent $[M\text{-}(NO_3)^-]^+$ peak in the mass spectra of the complexes corresponding to the loss of one nitrate anion.[65] The solution stability of the phen complexes **1** and **4** in 10% aqueous methanol has been evidenced from the mass spectra that show only the $[M\text{-}(NO_3)^-]^+$ peak in both cases implying that the heterocyclic bases are coordinated to the metal in an aqueous medium (Figures S1(a), S4(b) in the Supporting Information). The solution stability of the dppz complex **3** is also evidenced from its overall stability constant (β_2) value ($\log \beta_2 = 10.4$) in 10% aqueous DMF.[55] The IR spectral data indicate the presence of bidentate nitrate coordination from the appearance of a medium to strong intensity band at ∼1400 cm^{-1} suggesting the binding of the nitrate anions to the metal centers (Figures S7−S12 in the Supporting Information).[66] The ^1H NMR spectra of the diamagnetic La(III) complexes (**1**−**3**) in DMSO-d_6 show characteristic spectral features of metal-bound phenanthroline bases (Figures S13−S15 in the Supporting Information). The room temperature μ_{eff} values for **4**−**6** indicate paramagnetic ($4f^7$) nature of the Gd(III) complexes. The electronic absorption spectra of the complexes in DMF show a

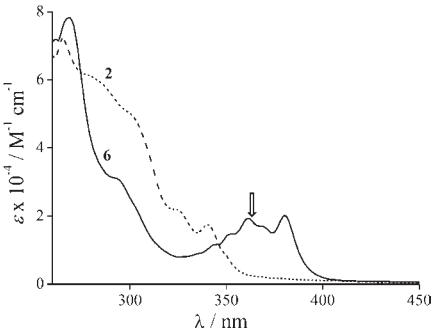

Figure 1. Electronic absorption spectra of $[La(dpq)_2(NO_3)_3]$ (**2**) and $[Gd(dppz)_2(NO_3)_3]$ (**6**) in DMF. Wavelength 365 nm used for DNA photocleavage experiments is shown by an arrow.

ligand centered $\pi \rightarrow \pi^*$ transition at ∼265 nm (Figure 1, Figure S16 in the Supporting Information). The dpq complexes **2** and **5** exhibit a band around 340 nm that could be due to $n \rightarrow \pi^*$ transition involving the quinoxaline moiety. The dppz complexes **3** and **6** show two bands at 361 and 380 nm assignable to the $n \rightarrow \pi^*$ transitions of the phenazine moiety.[48] Absorption spectral traces of complex $[La(dppz)_2(NO_3)_3]$ (**3**) in 10% aqueous DMF solution at an interval of 15 min and monitored up to 5 h do not show any significant spectral change (Figure S17 in the Supporting Information). The fluorescence emission spectra of the complexes in DMF at a complex concentration of 25 and 50 μM show a very weak emission at 420 nm when excited at 361 nm. The crystal structures of the phen complexes **1** and **4** are known in the literature.[67,68] In the solid state structure of $[Ln(B)_2(NO_3)_3]$, the La(III) and Gd(III) ions are known to bind four nitrogen atoms of two phen ligands and six oxygen atoms of three bidentate chelating nitrate ligands in a distorted bicapped dodecahedron LnN_4O_6 geometry. The complexes **1** − **6** are structurally similar as evidenced from their IR data. The complexes, however, exist as $[Ln(B)_2(NO_3)_2](NO_3)$ as the major species in a solution phase as evidenced from the mass spectral and conductivity data. The dpq and dppz complexes are redox active showing ligand reduction in DMF-0.1 M TBAP (Figure S18−S20 in the Supporting Information). The dppz complexes **3** and **6** show a cathodic response near −1.1 V (E_{pc}) with two

(65) Bünzli, J. C. G.; Merbach, A. E.; Nielson, R. M. *Inorg. Chim. Acta* **1987**, *139*, 151.
(66) (a) Nakamoto, K. *Infrared and Raman Spectra of Inorganic and Coordination Compounds*, 4th ed., Wiley: New York, 1986. (b) Curtis, N. F.; Curtis, Y. M. *Inorg. Chem.* **1968**, *4*, 801.
(67) Frechette, M.; Butler, I. R.; Hynes, R.; Detellier, C. *Inorg. Chem.* **1992**, *31*, 1650.
(68) Rybacov, V. B.; Zakharov, V. N.; Kamyshnyi, A. L.; Aslanov, L. A.; Suisalo, A. P. *Koord. Khim.* **1991**, *17*, 1061.

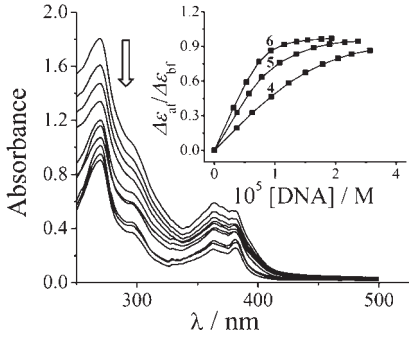

Figure 2. Absorption spectral traces of complex **6** in 5 mM Tris-HCl buffer (pH 7.2) on increasing the quantity of CT DNA with the inset showing the least-squares fit of $\Delta\varepsilon_{af}/\Delta\varepsilon_{bf}$ versus [DNA] for $[Gd(phen)_2(NO_3)_3]$ (**4**), $[Gd(dpq)_2(NO_3)_3]$ (**5**), and $[Gd(dppz)_2(NO_3)_3]$ (**6**) using the MvH equation (vide text).

anodic counterparts near −1.0 V (E_{pa1}) and −0.2 V (E_{pa2}) with i_{pa}/i_{pc} current ratio of ∼0.6 and ∼0.2, respectively. The redox data indicate the instability of the reduced species following ECE mechanism.[69] The dppz ligand alone shows a quasi-reversible voltammogram at −1.15 V with a ΔE_p value of 70 mV and i_{pa}/i_{pc} ratio of 0.9 at 50 mV s^{-1}. The dpq complexes **2** and **5** show cathodic peak near −1.4 V with poor reversibility possibly because of instability of the reduced species. The redox processes are primarily due to ligand reductions. The phenanthroline complexes are redox inactive.

DNA Binding. Absorption titration technique has been used to monitor the mode of interaction of the complexes **1**−**6** with CT DNA (Figure 2, Figure S21 in the Supporting Information). The intrinsic equilibrium DNA binding constant (K_b) values of the complexes along with the binding site size (s) are given in Table 2. The K_b values of $\sim 10^5$ M^{-1} follow the order: **3, 6** (dppz) > **2, 5** (dpq) > **1, 4** (phen). The dppz complexes show higher K_b values in comparison to their dpq and phen analogues possibly because of the presence of an extended aromatic moiety in dppz.[70] The s value, which is a fitted parameter in the MvH equation, gives a measure of the number of DNA bases associated with the complex and s value of <1 typically arises because of aggregation of hydrophobic molecules on the DNA surface.[71] The greater value of s for the dppz complex in comparison to those for the dpq and phen complexes indicates better DNA binding propensity of the dppz complexes. We have used a fluorescence spectral titration method to obtain the apparent binding constant values (K_{app}) of the complexes **1**−**6** (Table 2, Figures S22, S23 in the Supporting Information). Ethidium bromide has been used as a spectral probe as it exhibits enhanced emission intensity when it binds to the DNA. The competitive binding of the complexes to DNA could result in the displacement of the bound ethidium bromide and could cause decrease in the emission intensity because of solvent quenching. The K_{app} values of the complexes are $\sim 10^6$ M^{-1}.

Thermal denaturation measurements have been carried out to gain insights into the binding of the complexes **1**−**6** to CT DNA (Table 2, Figure 3(a), Figure S24(a) in the Supporting Information). A small positive shift of DNA melting temperature (ΔT_m) is observed upon addition of the complex to CT DNA. The low ΔT_m values suggest primarily groove binding nature of the complexes to CT DNA stabilizing DNA double helix structure in preference to an intercalative mode of binding to DNA that normally gives a large positive ΔT_m value.[72] Viscosity measurements have been carried out to examine the effect of the complexes on the specific relative viscosity of DNA (Figure 3(b) and Figure S24(b) in the Supporting Information). Since the relative specific viscosity (η/η_0) of DNA gives a measure on the increase in contour length associated with the separation of DNA base pairs caused by intercalation, a classical DNA intercalator like ethidium bromide shows a significant increase in the viscosity of the DNA solutions (η and η_0 are the specific viscosities of DNA in the presence and absence of the complexes, respectively). In contrast, a partial and/or non-intercalation of the complex could result in less pronounced effect on the viscosity.[73] The groove binder Hoechst 33258 has been used as a reference compound that shows almost no apparent change in viscosity. The results indicate that the complexes are possibly DNA groove binders with the dppz complex showing a partial intercalative binding mode.[74]

Photonuclease Activity. Photoinduced DNA cleavage activity of the complexes **1**−**6** has been studied using SC pUC19 DNA (30 μM, 0.2 μg) in a medium of Tris-HCl/NaCl (50 mM, pH, 7.2) buffer on irradiation with a low power monochromatic UV-A light of 365 nm (6W) (Table 3, Figure 4). The phen complexes **1** and **4** do not have any photoactive ligand moiety. Both the phen complexes are poor cleavers of DNA in UV-A light. The dpq and dppz complexes with respective photoactive quinoxaline and phenazine moiety show significant photoinduced DNA cleavage activity in nanomolar complex concentration. The dppz complexes **3** and **6** on photoirradiation at 365 nm for 2 h show ∼90% cleavage of SC DNA to its NC form at a complex concentration of 800 nM (lanes 8, 11 in Figure 4). The dpq complexes show ∼85% cleavage of SC DNA under similar conditions (lanes 7, 10 in Figure 4). The photocleavage of DNA by the complexes has been found to be time dependent showing higher cleavage activity on longer exposure time (Figures S25, S26 in the Supporting Information). Furthermore, the complexes at 5 μM concentration could cleave DNA completely for an exposure time of 25 min (Figure S27 in the Supporting Information). The control experiment with only SC DNA exposed to 365 nm light does not show any cleavage of DNA. The ligands or the metal salt alone do not show any significant DNA cleavage activity under similar reaction conditions (Figure 4). As mentioned earlier, lanthanides are well-known to show hydrolytic DNA cleavage activity.[4] Control experiments have been done using SC DNA in the presence of **1**−**6** in dark. We have not observed any hydrolytic DNA cleavage activity of the complexes at the concentration that has been used

(69) Nicholson, R. S.; Shain, I. *Anal. Chem.* **1965**, *37*, 190.
(70) Phillips, T.; Haq, I.; Meijer, A. J. H. M.; Adams, H.; Soutar, I.; Swanson, L.; Sykes, M. J.; Thomas, J. A. *Biochemistry* **2004**, *43*, 13657.
(71) Angeles-Boza, A. M.; Bradley, P. M.; Fu, P. K.-L; Wicke, S. E.; Bacsa, J.; Dunbar, K. R.; Turro, C. *Inorg. Chem.* **2004**, *43*, 8510.
(72) (a) An, Y.; Liu, S.-D.; Deng, S.-Y.; Ji, L.-N.; Mao, Z.-W. *J. Inorg. Biochem.* **2006**, *100*, 1586. (b) Gunther, L. E.; Yong, A. S. *J. Am. Chem. Soc.* **1968**, *90*, 7323.
(73) Veal, J. M.; Rill, R. L. *Biochemistry* **1991**, *30*, 1132.
(74) Pellegrini, P. P.; Aldrich-Wright, J. R. *Dalton Trans.* **2003**, 176.

Table 2. DNA Binding and BSA Stern−Volmer Quenching data for the Complexes **1**−**6**

Complex	K_b/M^{-1} [s][a]	K_{app}[b]/M^{-1}	ΔT_m[c]/ °C	K_{BSA}[d]/M^{-1}
$[La(phen)_2(NO_3)_3]$ (**1**)	$5.7(\pm0.3) \times 10^4$ [0.1]	4.0×10^5	0.8	7.0×10^4
$[La(dpq)_2(NO_3)_3]$ (**2**)	$3.0(\pm0.2) \times 10^5$ [0.3]	1.4×10^6	1.8	2.0×10^5
$[La(dppz)_2(NO_3)_3]$ (**3**)	$5.2(\pm0.6) \times 10^5$ [0.4]	3.4×10^6	3.2	3.3×10^5
$[Gd(phen)_2(NO_3)_3]$ (**4**)	$6.2(\pm0.2) \times 10^4$ [0.1]	5.0×10^5	0.9	7.4×10^4
$[Gd(dpq)_2(NO_3)_3]$ (**5**)	$3.6(\pm0.4) \times 10^5$ [0.3]	2.2×10^6	1.9	2.5×10^5
$[Gd(dppz)_2(NO_3)_3]$ (**6**)	$5.8(\pm0.7) \times 10^5$ [0.4]	4.3×10^6	3.3	3.5×10^5

[a] K_b, DNA binding constant (*s*, binding site size). [b] K_{app}, apparent DNA binding constant. [c] Change in the DNA melting temperature. [d] K_{BSA}, Stern−Volmer quenching constant for BSA fluorescence. The K_{BSA} values for $La(NO_3)_3 \cdot 6H_2O$, $Gd(NO_3)_3 \cdot 6H_2O$, phen, dpq and dppz are 6.8×10^3, 7.1×10^3, 4.7×10^4, 6.5×10^4 and 9.6×10^4 M^{-1}, respectively.

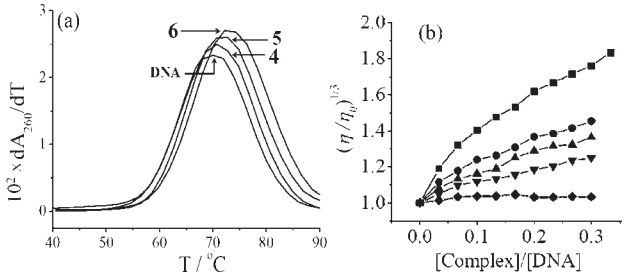

Figure 3. (a) Thermal denaturation plots of 180 μM CT DNA alone and on addition of the gadolinium(III) complexes **4**−**6**. (b) Effect of increasing the concentration of the complexes $[Gd(phen)_2(NO_3)_3]$ (**4**,▼), $[Gd(dpq)_2(NO_3)_3]$ (**5**, ▲), $[Gd(dppz)_2(NO_3)_3]$ (**6**, ●), ethidium bromide (EB, ■), and Hoechst 33258 (♦) on the relative viscosities of CT-DNA at 37.0(±0.1) °C in 5 mM Tris-HCl buffer (pH 7.2) containing 2.5−20% DMF, [DNA] = 150 μM.

Table 3. Photo-Induced SC DNA (0.2 μg, 33.3 μM) Cleavage Data[a] at 365 nm

Sl. No.	reaction condition	[complex]/ *n*M	*t*/ h	%NC
1.	DNA control		2	3
2.	DNA + $[La(dpq)_2(NO_3)_3]$ (**2**) (in dark)	800	2	6
3.	DNA + $[La(phen)_2(NO_3)_3]$ (**1**)	800	2	23
4.	DNA + $[La(dpq)_2(NO_3)_3]$ (**2**)	800	2	81
5.	DNA + $[La(dppz)_2(NO_3)_3]$ (**3**)	800	2	86
6.	DNA + $[Gd(phen)_2(NO_3)_3]$ (**4**)	800	2	26
7.	DNA + $[Gd(dpq)_2(NO_3)_3]$ (**5**)	800	2	85
8.	DNA + $[Gd(dppz)_2(NO_3)_3]$ (**6**)	800	2	91

[a] Exposure time, *t*. SC and NC are supercoiled and nicked circular forms of pUC19 DNA. Additional pUC19 DNA cleavage data for the ligands (1.6 μM) and metal salts (5 μM) giving %NC for 2 h photoexposure time: dpq, 16%; dppz, 18%; $La(NO_3)_3$, 9%; $Gd(NO_3)_3$, 7%. Additional %NC data for 30 min photoexposure time for ligands having 10 μM concentration: dpq, 26%; dppz 31%.

for the photoinduced DNA cleavage experiments. The DNA groove binding propensity of the complexes has been studied using DNA minor groove binder distamycin-A and the major groove binder methyl green (Figure 4). Distamycin-A (50 μM) alone shows ~15% cleavage of SC DNA (30 μM) to its NC form at 365 nm on 2 h photoexposure. Addition of the dpq complex to distamycin-A bound SC DNA causes significant inhibition in the photocleavage activity. The dppz complex displays no apparent inhibition in the presence of distamycin-A, but significant inhibition is observed with methyl green bound DNA (Figure 4). The data suggest minor and major groove binding preferences of the dpq and dppz complexes, respectively.[70,75]

Mechanistic Studies. The mechanistic aspects of the UV-A light-induced DNA cleavage reactions of **3** and **6** have been studied using different additives (Figure 5, Figure S28 in the Supporting Information). The complexes are cleavage inactive in UV-A light of 365 nm under argon atmosphere indicating the necessity of reactive oxygen species (ROS) for the DNA cleavage. The DNA cleavage reactions involving molecular oxygen could involve two major mechanistic pathways, namely, the type-II process forming singlet oxygen species or a photoredox pathway forming reactive hydroxyl radicals. Addition of singlet oxygen quenchers such as sodium azide, TEMP, or DABCO to SC DNA partially inhibits the photoinduced DNA cleavage activity. Hydroxyl radical scavengers like DMSO or catalase also show partial inhibition in the DNA cleavage. The results suggest the involvement of both singlet oxygen ($^1O_2$) and hydroxyl radicals as ROS. The formation of singlet oxygen is also evidenced from the reaction in D_2O showing enhancement of the cleavage activity because of longer lifetime of $^1O_2$ in this medium.[76] While the involvement of the quinoxaline/phenazine moiety of the photoactive phenanthroline bases is likely to generate the singlet oxygen species in a type-II process, the formation of hydroxyl radicals involving transient Ln(IV) species, as suggested by Parker and co-workers, seems unlikely considering redox inactive nature of the metal ions.[49]

Protein Binding Study. The interaction of **1**−**6** with bovine serum albumin (BSA) has been studied from tryptophan emission-quenching experiments. The fluorescence intensity of BSA is mainly due to the tryptophan residues Trp-134 and Trp-212. The changes in the emission spectra of tryptophan in BSA are primarily due to change in protein conformation, subunit association, substrate binding, or denaturation.[77] Emission intensity of BSA is found to gradually decrease on increasing the complex concentration. The quenching constant (K_{BSA}) value has been determined quantitatively by using the Stern−Volmer equation.[78] The K_{BSA} values of 10^4−10^5 M^{-1} indicate good BSA interaction propensity of the complexes (Figures S29, S30 in the Supporting Information). The K_{BSA} values follow the order: **3, 6** (dppz) > **2, 5** (dpq) > **1, 4** (phen). The higher BSA emission quenching propensity of the dppz complexes

(75) (a) Erkkila, K. E.; Odom, D. T.; Barton, J. K. *Chem. Rev.* **1999**, *99*, 2777. (b) Delaney, S.; Pascaly, M.; Bhattacharya, P. K.; Han, K.; Barton, J. K. *Inorg. Chem.* **2002**, *41*, 1966.

(76) (a) Khan, A. U. *J. Phys. Chem.* **1976**, *80*, 2219. (b) Merkel, P. B.; Kearns, D. R. *J. Am. Chem. Soc.* **1972**, *94*, 1029.

(77) (a) Wang, Y.-Q.; Zhang, H.-M.; Zhang, G.-C.; Tao, W.-H.; Tang, S.-H. *J. Lumin.* **2007**, *126*, 211. (b) Sarkar, B. *Biol. Trace Elem. Res.* **1989**, *21*, 137.

(78) Lakowicz, J. R. *Principles of Fluorescence Spectroscopy*, 2nd ed.; Plenum Press: New York, 1999.

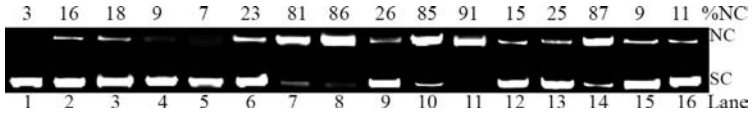

Figure 4. Cleavage of SC pUC19 DNA (0.2 μg, 30 μM) by the complexes **1**−**6** (800 nM) in 50 mM Tris-HCl/NaCl buffer (pH, 7.2) containing 10% DMF on photoirradiation at 365 nm (6 W) for 2 h exposure: lane 1, DNA control; lane 2, DNA + dpq (1.6 μM); lane 3, DNA + dppz (1.6 μM); lane 4, DNA + $La(NO_3)_3$ (5 μM); lane 5, DNA + $Gd(NO_3)_3$ (5 μM); lanes 6−11, DNA + complexes **1**−**6**, respectively; lane 12, DNA + distamycin-A (50 μM); lane 13, DNA + distamycin-A (50 μM) + **5**; lane 14, DNA + distamycin-A (50 μM) + **6**; lane 15, DNA + methyl green (200 μM); lane 16, DNA + methyl green (200 μM) + **6**.

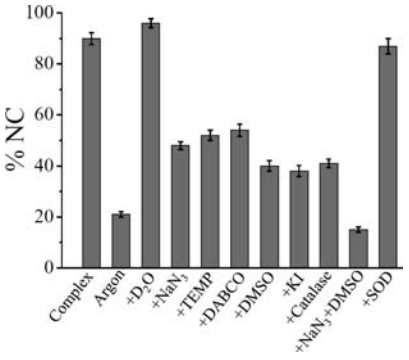

Figure 5. Cleavage of SC pUC19 DNA (0.2 μg, 30 μM) by $[Gd(dppz)_2(NO_3)_3]$ (**6**) in the presence of various additives in Tris-HCl buffer containing 10% DMF. The complex concentration and exposure time for UV-A light (365 nm) experiments are 800 nM and 2 h, respectively. The additive concentrations/quantities are sodium azide, 0.5 mM; KI, 0.5 mM; TEMP, 0.5 mM; DABCO, 0.5 mM; D_2O, 16 μL; DMSO, 4 μL; catalase, 4 units; SOD, 4 units.

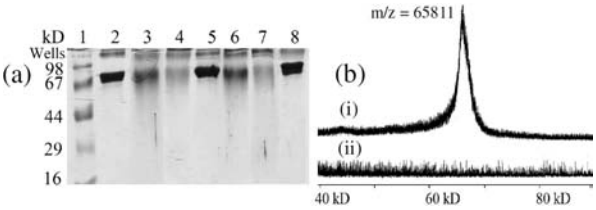

Figure 6. Photocleavage of bovine serum albumin (BSA, 5 μM) in UV-A light of 365 nm by $[Gd(dppz)_2(NO_3)_3]$ (**6**) in 50 mM Tris-HCl buffer having 0.6% DMF (pH 7.2). Panel (a) shows complexes **3** and **6** in 12.5% SDS-PAGE (t = exposure time of 15 or 30 min): lane 1, molecular marker; lane 2, BSA control (30 min); lane 3, BSA + **3** (15 μM, 15 min); lane 4, BSA + **3** (15 μM, 30 min); lane 5, BSA + **3** (15 μM, in dark); lane 6, BSA + **6** (15 μM, 15 min); lane 7, BSA + **6** (15 μM, 30 min); lane 8, BSA + **6** (15 μM, in dark). Panel (b) shows the MALDI spectra on BSA + dppz complex **6** in dark (i) and after exposure to UV-A light of 365 nm for 30 min (ii).

could be due to better hydrophobic nature of dppz than dpq and phen ligands. The phen, dpq, and dppz ligands under similar experimental conditions show lower binding propensity to BSA (Table 2, Figure S31 in the Supporting Information).

Protein Cleavage Activity. We have investigated the UV-A (365 nm) light-induced protein cleavage activity of the complexes **1**−**6** using 5 μM BSA in Tris-HCl buffer containing 0.6% DMF by SDS-PAGE (Figure 6, Figures S32, S33 in the Supporting Information). At complex concentration of 15 μM, the dppz complexes **3** and **6** show complete degradation of BSA when exposed to light for 30 min. Complexes **3** and **6** do not show any protein cleavage activity in dark thus ruling out any hydrolytic protein damage. The phen (**1**, **4**) and dpq (**2**, **5**) complexes are found to be inactive in cleaving the protein on photoexposure to UV-A light. The dppz ligand shows significantly lower BSA photocleavage activity than the dppz complexes, while phen and dpq ligands are cleavage inactive (Figure S34 in the Supporting Information). The involvement of reactive oxygen species (ROS) in the cleavage reaction has been evidenced from the cleavage reactions in the presence of additives like singlet oxygen quenchers NaN_3 (3 mM) and TEMP (3 mM) and hydroxyl radical scavengers like DMSO (20 μL) and KI (3 mM). Both NaN_3 and TEMP do not show any apparent effect on the photoinduced protein cleavage activity of **3** and **6** thus excluding the possibility of singlet oxygen ($^1O_2$) pathway. Addition of DMSO and KI causes significant reduction in the protein photocleavage activity suggesting the involvement of hydroxyl radicals as the reactive species (Figure S35 in the Supporting Information). The dppz complex with BSA in dark shows a mass peak of 65.8 kD for the protein. The sample on exposure to UV-A light for 30 min shows complete degradation of the protein and no significant peak is observed in the mass spectrum (Figure 6). The dpq complexes do not show any photocleavage of BSA under similar reaction conditions (Figure 6).

Cell Cytotoxicity. Cell photocytotoxicity of the dppz complexes **3** and **6** has been studied in human cervical carcinoma (HeLa) cells using MTT assay. The dppz complexes **3** and **6** upon prior incubation for 4 h in dark and subsequent photoexposure to UV-A light (365 nm) for 15 min show a dose-dependent decrease in cell viability with an IC_{50} value of 341 nM and 573 nM, respectively (Figure 7 (a), Table 4, Figure S36 in the Supporting Information). The cells unexposed to light gave an IC_{50} value of >100 μM for both **3** and **6**. Interestingly, the dppz ligand alone shows significant dark cytotoxicity (IC_{50} value of 11.6 μM) upon incubation for 24 h in dark and in UV-A light of 365 nm (IC_{50} value of 413 nM) upon 4 h incubation in dark followed by exposure to UV-A light (Figure 7 (b), Table 4). No reduction in cell viability was observed upon incubation of the cells with complexes **3** and **6** in dark for 24 h. Hence the binding of Ln(III) ions to dppz is found to significantly decrease the dark toxicity of the dppz ligand. The lanthanide ions could thus moderate the dark toxicity of photoactive organic antitumor agents having phenazine moiety for phototherapeutic applications. Cisplatin was used as a control for assessing the dark toxicity. Cisplatin gave an IC_{50} value of 7.5 μM in HeLa on 24 h incubation (Table 4, Figure S37 in the Supporting Information). Whereas on 4 h incubation of the HeLa cells with cisplatin in dark followed by photoexposure to UV-A light, the IC_{50} values were 71.3 μM in dark and 68.7 μM in UV-A light-exposed cells (Figure S38 in the Supporting Information). Photofrin is known to have an IC_{50} value of 4.3 ± 0.2 μM on

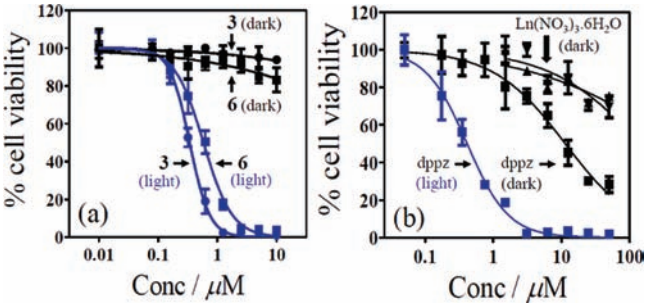

Figure 7. (a) Photocytotoxicity of the dppz complexes **3** and **6** in HeLa cells on 4 h incubation in dark followed by exposure to UV-A light (365 nm, 15 min) as determined by MTT assay. The dark-treated and photoexposed cells for complex **3** are shown by black-circles and blue-circles, respectively. For complex **6**, it is shown by black-squares and blue-squares, respectively. (b) Controls: dppz ligand exposed to UV-A light (365 nm, 15 min) (blue squares), dppz ligand in dark (black squares), $La(NO_3)_3 \cdot 6H_2O$ in dark (▲) and $Gd(NO_3)_3 \cdot 6H_2O$ in dark (▼).

Table 4. Comparison of the IC_{50} values (in HeLa cells) of Cisplatin, dppz ligand, and the dppz Complexes

compound	IC_{50} (light)[a]	IC_{50} (dark)[b]
$[La(dppz)_2(NO_3)_3]$ (**3**)	341 nM	$>100\ \mu$M
$[Gd(dppz)_2(NO_3)_3]$ (**6**)	573 nM	$>100\ \mu$M
$[Zn(dppz)_2(NO_3)_2]$	367 nM	22.4 μM
dppz	413 nM	11.6 μM
cisplatin	68.7 μM	7.5 μM

[a] The IC_{50} values correspond to 4 h incubation in dark followed by photoexposure to UV-A light (365 nm, 0.55 J cm^{-2}). [b] The IC_{50} values correspond to 24 h incubation in dark.

633 nm excitation (5 *J* cm^{-2}) and >41 μM in dark on HeLa cells.[79] To explore the role of lanthanide ions, we have prepared a zinc(II) complex of dppz ligand as a control.[80] The complex $[Zn(dppz)_2(NO_3)_2]$ gave an IC_{50} value of 367 nM in UV-A light in HeLa cells, while upon 24 h incubation in dark gave an IC_{50} value of 22.4 μM indicating significant dark toxicity of the complex (Figure S39 in the Supporting Information). While dark toxicity of the zinc(II) complex of dppz is slightly less to that of the free dppz ligand, a significant reduction in the dppz ligand dark toxicity is observed on binding to the lanthanide(III) ions, while retaining the photocytotoxic activity in UV-A light.

(79) Delaey, E.; Van Laar, F.; De Vos, D.; Kamuhabwa, A.; Jacobs, P.; De Witte, P. *J. Photochem. Photobiol., B* **2000**, *55*, 27.

(80) The Zn(II) dppz complex of formulation $[Zn(dppz)_2(NO_3)_2]$, used as a control in photocytotoxicity study, was prepared by reacting $Zn(NO_3)_2 \cdot 6H_2O$ (0.15 g; 0.5 mmol) with dppz (0.28 g; 1.0 mmol) in MeCN-MeOH at 0 °C and was isolated as a light yellow solid in ~68% yield. Analytical data: Calcd for $C_{36}H_{20}N_{10}O_6Zn$: C, 57.35; H, 2.67; N, 18.58. Found: C, 57.68; H, 2.83; N, 18.44. ESI-MS in MeCN: *m*/*z* 691 $[M - NO_3^-]^+$.

Conclusions

In summary, we present the first systematic study on photoinduced DNA and protein cleavage activity of lanthanide complexes having *N*,*N*-donor phenanthroline bases. The photocytotoxic property of two dipyridophenazine complexes in UV-A light is reported. The diamagnetic La(III) and paramagnetic Gd(III) complexes of phenanthroline bases having LaO_6N_4 and GdO_6N_4 core show good DNA and protein binding propensity. The dpq and dppz complexes display highly efficient photoinduced DNA cleavage activity at 365 nm following singlet oxygen and hydroxyl radical pathways at nanomolar complex concentration. The DNA cleavage observed at nanomolar concentration is significant for metal-based photocleavers of DNA. The dppz complexes show photocleavage of BSA at 15 μM complex concentration. The observation of low dark cytotoxicity and high photocytotoxicity of the dppz complexes in UV-A light in HeLa cells is of importance toward designing and developing new lanthanide complexes as potent photoactivatable anticancer agents. Binding of the lanthanide ions to dppz is found to significantly reduce the dark toxicity of the ligand and marginally enhances its photocytotoxicity. Lanthanide ions could act as a carrier of photocytotoxic organic molecules like dppz for potential phototherapeutic applications.

Acknowledgment. We thank the Department of Science and Technology (DST), Government of India, for financial support (SR/S5/MBD-02/2007). A.R.C. thanks the DST for the J. C. Bose national fellowship. A.H. and S.S. thank CSIR for research fellowships.

Supporting Information Available: Mass, infrared, electronic and ^1H NMR spectra, cyclic voltammograms, DNA and protein binding, DNA and protein photocleavage diagrams, and MTT assay plots (Figures S1−S39). This material is available free of charge via the Internet at http://pubs.acs.org.